

Theory of the structural phase transition of GeTe

K. M. Rabe and J. D. Joannopoulos

Department of Physics, Massachusetts Institute of Technology, Cambridge, Massachusetts 02139

(Received 8 December 1986)

A completely *ab initio* theoretical investigation of the rocksalt-rhombohedral structural phase transition of GeTe is described. Starting from an anharmonic lattice Hamiltonian, a model Hamiltonian that includes coupling of the order parameter to long-wavelength strain is constructed. The parameters appearing in the model are calculated using the self-consistent *ab initio* pseudopotential total-energy method. The phase transition in the model system is studied through a momentum-space renormalization-group-theory approach, leading to the prediction of a fluctuation driven first-order transition at 657 ± 100 K. The strain coupling is found to be crucial in determining the first-order character of the transition. A discussion of approximations made in this approach and considerations relevant to its application to structural transitions in other systems is included.

I. INTRODUCTION

In the application of modern concepts of critical phenomena to the study of finite-temperature phase transitions in real materials, the calculation of the transition temperature and other nonuniversal critical properties is essential. This requires the combination of detailed microscopic quantitative knowledge of the properties of the material under consideration with an appropriate statistical mechanical treatment.

One way to obtain these properties is through first-principles total-energy calculations. Previous attempts to calculate transition temperatures^{1,2} have used total energy methods which rely on approximations limiting their accuracy and range of applicability. In contrast, the *ab initio* pseudopotential method has been seen to be highly accurate in describing the zero-temperature structural properties of a wide variety of systems,³ including group-IV tellurides.⁴ In the present study of the structural phase transition of bulk GeTe, we combine this self-consistent method with a renormalization-group-theory (RG) approach to calculate T_c and predict other critical phenomena associated with the transition, in excellent agreement with available experimental data.

At high temperatures the IV-VI narrow-gap semiconductor GeTe has the rocksalt structure. At low temperatures the system exists in a rhombohedral structure. This structure, shown in Fig. 1, can be described as a rocksalt structure slightly distorted by freezing in a $\mathbf{k}=0$ optic phonon along the [111] direction, corresponding to the order parameter of the transition, with a subsequent shear relaxation along [111], corresponding to the secondary order parameter. Experimental studies of the transition and their interpretation are somewhat difficult because of the high transition temperature and intrinsic limitations on the quality of the sample. The latter arises because the compound GeTe is not in the range of homogeneity of the alloy, which for a nominal stoichiometric composition results in the coexistence of free Ge with a 50.3 at. % Te phase.⁵⁻⁷ This phase exhibits the rhombohedral-rocksalt transition and contains

free holes arising mainly from Ge vacancies. The temperature dependence of the order parameter near the transition has not been observed, as it has in the analogous compound SnTe using elastic neutron scattering.⁸ However, transition temperatures in the range 625–700 K have been extracted from measurements of the temperature dependence of the volume and rhombohedral angle α using x-ray diffraction,^{6,9-11} calorimetric determinations of the heat evolution associated with the transition,¹² and studies of anomalies in the thermal expansion^{5,7,13-15} and electrical resistivity.^{16,17} In some measurements¹¹ small discontinuities in volume and α have been detected at the transition, suggesting that it may be weakly first order.

Our theoretical investigation of this transition proceeds in three steps. In Sec. II we show how to manipulate the full anharmonic lattice Hamiltonian into a form with a tractable number of coupling constants. In Sec. III we determine the coupling constants for GeTe using pseudopotential total-energy calculations for various structural configurations. Finally, in Sec. IV we describe a renormalization-group calculation implemented in momentum space which yields T_c and the critical properties associated with the transition. Section V contains a discussion of the approximations in this approach and the

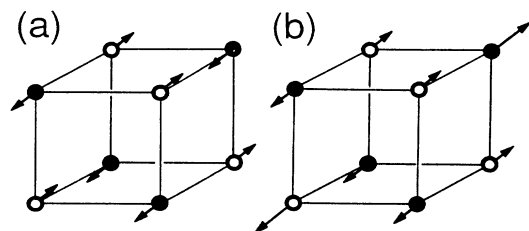


FIG. 1. The low-temperature rhombohedral structure of GeTe is obtained by two independent distortions of the rocksalt structure: (a) relative displacement of the Ge and Te sublattices by $\tau a_0(111)$ and (b) shear along [111] which reduces the rhombohedral angle α from its fcc value of 60° .

considerations relevant to its application to finite-temperature structural transitions in other systems, and concluding remarks.

II. CONSTRUCTION OF MODEL HAMILTONIAN

As the starting point of a first-principles study, we seek a microscopic Hamiltonian for the system which incorporates a correct description of the features leading to the structural transition.¹⁸ For GeTe, it is appropriate to use an anharmonic lattice Hamiltonian^{19,20} in which only the ionic degrees of freedom appear explicitly, and the electronic effects are included in the Born-Oppenheimer approximation. However, even if this Hamiltonian is simplified by expanding to fourth order about the prototype configuration (the rocksalt structure), it is still too complicated for calculating numerical values of the coefficients or for evaluating the partition function and obtaining thermal properties. The local-mode approximation²¹ provides an intuitively appealing way of obtaining an equivalent model Hamiltonian with a simpler form and a greatly reduced number of parameters. For each unit cell, the local-mode variable is defined as the projection of local ionic displacements onto the polarization vectors of the $\mathbf{k}=0$ optic modes, referred to the mean positions in the high-temperature structure. The Hamiltonian is expanded in symmetry allowed powers of the local mode variables, with on-site terms kept up to some arbitrary order and intersite interactions to quadratic order only.

To a large extent, the requirement that the local mode have the lattice symmetry restricts the possible definitions. The approximation of purely local anharmonicity, essential for obtaining a Hamiltonian with a small number of parameters, necessitates that the precise choice of local mode incorporate a physical understanding of the lattice instability. The charge flow and energy gain resulting from the symmetry breaking by the distortion of the six equivalent nearest-neighbor bonds of the rocksalt structure involves primarily Te p -like states,^{4,22} while the main anharmonic contribution to the energy originates in the nonlinear Te polarizability.²³ Thus, for GeTe, the best choice of local mode emphasizes the distortion of the Te ion environment:

$$\xi_i = a_0^{-1} \left[\Delta \mathbf{r}_{\text{Te}}^i - \sum_{\text{NN}j} \Delta \mathbf{r}_{\text{Ge}}^j / 6 \right],$$

where a_0 is the length of the side of the fcc conventional unit cell, NN denotes nearest neighbor, and the displacements $\Delta \mathbf{r}$ are measured relative to the rocksalt structure (see Fig. 2).

Before giving the explicit approximate expression for the model Hamiltonian H_{mod} which will be used in the calculation, we study its properties using the exact form, obtained from the relation:

$$\exp[-\beta H_{\text{mod}}(\{\xi_i\})] = \int \left[\prod_i (d\sigma_i) \right] \exp[-\beta H_{\text{lat}}(\{\xi_i\}, \{\sigma_i\})],$$

where

$$\sigma_i = a_0^{-1} \left[\Delta \mathbf{r}_{\text{Te}}^i + \sum_{\text{NN}j} \Delta \mathbf{r}_{\text{Ge}}^j / 6 \right]$$

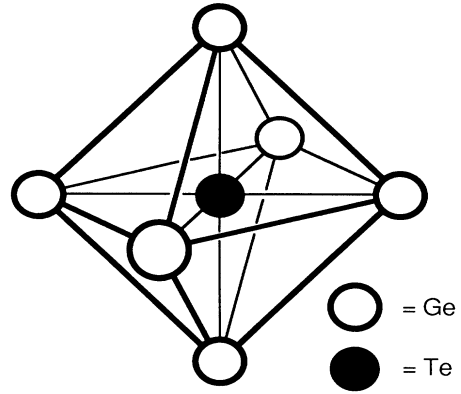


FIG. 2. The local-mode variable is defined as $\xi_i = a_0^{-1} (\mathbf{r}_{\text{Te}}^i - \sum_{\text{NN}j} \mathbf{r}_{\text{Ge}}^j / 6)$. The sum runs over the six nearest-neighbor Ge atoms, which in the rocksalt structure form an octahedron with the Te atom at the center.

and $H_{\text{lat}}(\{\xi_i\}, \{\sigma_i\})$ is the full anharmonic lattice Hamiltonian. We note that at fixed $\{\xi_i\}$, H_{mod} , in principle, depends on the energies of a $3N/2$ -dimensional space of ionic configurations and the temperature.

However, to a good approximation the situation is much simpler. We decompose H_{lat} as follows:

$$H_{\text{lat}}(\{\xi_i\}, \{\sigma_i\}) = H_1(\{\xi_i\}) + H_2(\{\sigma_i\}) + H_3(\{\xi_i\}, \{\sigma_i\}).$$

Because the physically important anharmonicity is associated with the $\{\xi_i\}$, it should be sufficient to include the $\{\sigma_i\}$ in the expansion of H_{lat} up to quadratic order only. The Gaussian integration over the $\{\sigma_i\}$ replaces $\{\sigma_i\}$ by the values which minimize H_{lat} at fixed $\{\xi_i\}$, and therefore the coefficients of H_{mod} are independent of temperature in this approximation.

The relation of $H_{\text{mod}}(\{\xi_i\})$ to the energies of ionic configurations $H_{\text{lat}}(\{\xi_i\}, \{\sigma_i\})$ can be further simplified by keeping only the lowest-order term in H_3 ,

$$\int d^3k V^{\alpha\beta}(\mathbf{k}) \sigma^\alpha(\mathbf{k}) \xi^\beta(-\mathbf{k}).$$

Then, with $\xi(\mathbf{k})$ nonzero, only the minimization with respect to the component of $\sigma(-\mathbf{k})$ which transforms according to the same representation of the group of \mathbf{k} is nontrivial. For small \mathbf{k} , however, $V(\mathbf{k})$ vanishes like k^2 , so there we keep instead the term proportional to

$$\int d^3k \int d^3k' V^{\alpha\beta\gamma\delta} k^\delta \sigma^\alpha(\mathbf{k}) \xi^\beta(\mathbf{k}') \xi^\gamma(\mathbf{k}-\mathbf{k}')$$

which describes the lowest-order coupling of ξ to long-wavelength strain. Rather than integrate this term out immediately, we will, for the time being, keep the long-wavelength strains explicitly in order to study the physics arising from this coupling.

The construction of H_{mod} for the GeTe transition proceeds as follows. The local-mode variables sit on the sites of an fcc lattice and only cubic-symmetry invariants

appear in the expansion of the Hamiltonian. We truncate the on-site potential at fourth order in the local-mode variable but keep isotropic terms to eighth order. Intersite interactions up to second order are included, since the constraints imposed by the sharing of Ge atoms by first- and second-neighbor local-mode octahedra suggest the coupling is important. The lowest-order terms involving long-wavelength strain fields are included explicitly, as discussed above.

$$-\frac{1}{2} \sum_i \left[\xi_x(\mathbf{R}_i) \left(a_1 \sum_{\mathbf{d} \in \{(\pm\hat{x}\pm\hat{y}), (\pm\hat{x}\pm\hat{z})\}} \xi_x(\mathbf{R}_i + a_0\mathbf{d}/2) + a_2 \sum_{\mathbf{d} \in \{(\pm\hat{y}\pm\hat{z})\}} \xi_x(\mathbf{R}_i + a_0\mathbf{d}/2) \right. \right. \\ \left. \left. + a_3 \sum_{\mathbf{d} \in \{(\pm\hat{x}\pm\hat{y})\}} (\mathbf{d}\cdot\hat{x})(\mathbf{d}\cdot\hat{y})\xi_y(\mathbf{R}_i + a_0\mathbf{d}/2) + a_3 \sum_{\mathbf{d} \in \{(\pm\hat{x}\pm\hat{z})\}} (\mathbf{d}\cdot\hat{x})(\mathbf{d}\cdot\hat{z})\xi_z(\mathbf{R}_i + a_0\mathbf{d}/2) \right) + \text{c.p.} \right],$$

where c.p. denotes cyclic permutation, and second-neighbor intersite interactions

$$-\frac{1}{2} \sum_i \left[\xi_x(\mathbf{R}_i) \left(b_1 \sum_{\mathbf{d} \in \{\pm\hat{x}\}} \xi_x(\mathbf{R}_i + a_0\mathbf{d}) + b_2 \sum_{\mathbf{d} \in \{\pm\hat{y}, \pm\hat{z}\}} \xi_x(\mathbf{R}_i + a_0\mathbf{d}) \right) + \text{c.p.} \right],$$

where $\xi(\mathbf{R}_i)$ is the local-mode variable at the fcc lattice site \mathbf{R}_i .

With the strain tensor $\vec{e}_{\alpha\beta} = (\delta u_\beta / \delta x_\alpha + \delta u_\alpha / \delta x_\beta) / 2$, the lowest-order terms which describe long-wavelength strain deformations and their coupling to the order parameter are

$$(\Omega_0)^{-1} \int d^3r \left[C_{11} \sum_{\alpha} e_{\alpha\alpha}^2(\mathbf{r}) / 2 + C_{12} \sum_{\substack{\alpha, \beta \\ \alpha \neq \beta}} e_{\alpha\alpha}(\mathbf{r}) e_{\beta\beta}(\mathbf{r}) / 2 + C_{44} \sum_{\substack{\alpha, \beta \\ \alpha \neq \beta}} e_{\alpha\beta}^2(\mathbf{r}) \right. \\ \left. - g_0 \sum_{\alpha} e_{\alpha\alpha}(\mathbf{r}) |\xi_i|^2 / 3 - g_1 \sum_{\substack{\alpha, \beta \\ \alpha < \beta}} e_{\alpha\beta}(\mathbf{r}) \xi_{i,\alpha} \xi_{i,\beta} - g_2 \sum_{\alpha} e_{\alpha\alpha}(\mathbf{r}) (\xi_{i,\alpha}^2 - |\xi_i|^2 / 3) \right].$$

These expressions define the model Hamiltonian coefficients A , u_0 , v_0 , D , E , a_1 , a_2 , a_3 , $b_1 + 2b_2$, C_{11} , C_{12} , C_{44} , g_0 , g_1 , and g_2 which will be calculated in Sec. III.

III. TOTAL-ENERGY CALCULATIONS

The values of the coefficients for GeTe are obtained by fitting the model Hamiltonian to the energies of a variety of local-mode configurations. For the zero-strain coefficients A , u_0 , v_0 , D , E , a_1 , a_2 , a_3 , and $b_1 + 2b_2$ we must consider configurations with the full fcc translational symmetry [Fig. 3(a)] as well as configurations with two translationally inequivalent types of local-mode variables on fcc lattice sites. For the fcc lattice, there are only two ways to divide the sites into two inequivalent classes, giving rise to an arrangement with a tetragonal unit cell [Fig. 3(b)] and to one with a rhombohedral unit cell [Fig. 3(c)]. In each type of unit cell we study two families of local-mode configurations, specified by a fixed polarization vector at each inequivalent site and a varying amplitude τ . For each family the energy as a function of τ determines one combination of coefficients at each order. Unfortunately, the second-neighbor couplings b_1 and b_2 cannot be separately determined without using still larger unit cells.

To obtain the strain coefficients C_{11} , C_{12} , C_{44} , g_0 , g_1 , and g_2 , it is sufficient to consider configurations in which the local mode is uniform and only the lattice changes. We study three types of variation corresponding to pure volume change ($e_{xx} = e_{yy} = e_{zz}$), pure rhombohedral angle change at fixed volume ($e_{xx} = e_{yy} = e_{zz}$, $e_{xy} = e_{yz} = e_{xz}$),

Carrying out this construction, we obtain the following explicit form for H_{mod} . The expression for the onsite potential is

$$\sum_i \left[A |\xi(\mathbf{R}_i)|^2 + u_0 |\xi(\mathbf{R}_i)|^4 + v_0 \sum_{\alpha} \xi_{\alpha}(\mathbf{R}_i)^4 \right. \\ \left. + D |\xi(\mathbf{R}_i)|^6 + E |\xi(\mathbf{R}_i)|^8 \right],$$

with the first-neighbor intersite interactions

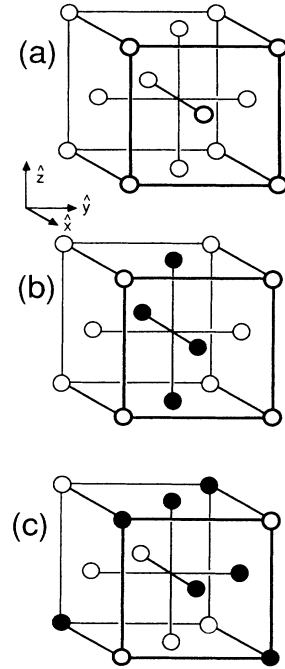


FIG. 3. The translational symmetries of the various local-mode configurations studied are illustrated. An fcc lattice with all sites equivalent is shown in (a). The division of lattice sites into two inequivalent types, as indicated by solid and open circles, yields (b) a tetragonal unit cell with equivalent sites lying in (010) planes, and (c) a rhombohedral unit cell with equivalent sites lying in (111) planes.

TABLE I. Specifications of the families of local-mode configurations for which total energies were calculated, the combinations of quadratic parameters determined, and the two Monkhorst-Pack (Ref. 29) \mathbf{k} -point sets used to study convergence. Open and solid circles are used to label translationally inequivalent lattice sites (see Fig. 3).

Configuration	Unit cell type	Local-mode variables		Quadratic parameters determined	k-point sets (number of points in full BZ)
		Open circles	Solid circles		
(a)	fcc	$\tau(111)$		$A + 4a_1 + 2a_2 + b_1 + 2b_2$	125,343
(b)	fcc	$\tau(010)$		$A + 4a_1 + 2a_2 + b_1 + 2b_2$	125,343
(c)	tetragonal	$\tau(010)$	$-\tau(010)$	$A - 4a_1 + 2a_2 + b_1 + 2b_2$	48,100
(d)	tetragonal	$\tau(101)$	$-\tau(101)$	$A - 2a_2 + b_1 + 2b_2$	48,100
(e)	rhombohedral	$\tau(111)$	$-\tau(111)$	$A - 4a_3 - b_1 - 2b_2$	27,125
(f)	rhombohedral	$\tau(112)$	$-\tau(112)$	$A + 2a_3 - b_1 - 2b_2$	27,125

and uniaxial strain (e_{zz}). The coefficients C_{11} , C_{12} , and C_{44} are obtained from configurations with $\tau=0$, while for g_0 , g_1 , and g_2 a configuration with nonzero τ must be included at each e .

As discussed in Sec. II, the local-mode configuration energy can be taken as the minimum over the energies of ionic configurations with the same translational and point symmetries. The types of zero-strain ionic configurations for which we must calculate the energy are specified in Table I and Fig. 4. For families (a), (b), (e), and (f) the choice of τ and the symmetry requirement completely

specify the ionic configuration. For families (c) and (d), the symmetry requirement is less restrictive, resulting in a one-dimensional space of ionic configurations, here labeled by σ , which must be searched for the energy minimum.

The necessary calculations of the energies of ionic configurations are performed using the self-consistent *ab initio* pseudopotential total-energy method.^{24,25} We use the spin-orbit averaged relativistic nonlocal atomic pseudopotentials for Ge and Te given by Bachelet, Hamann, and Schlüter.²⁶ Exchange and correlation are

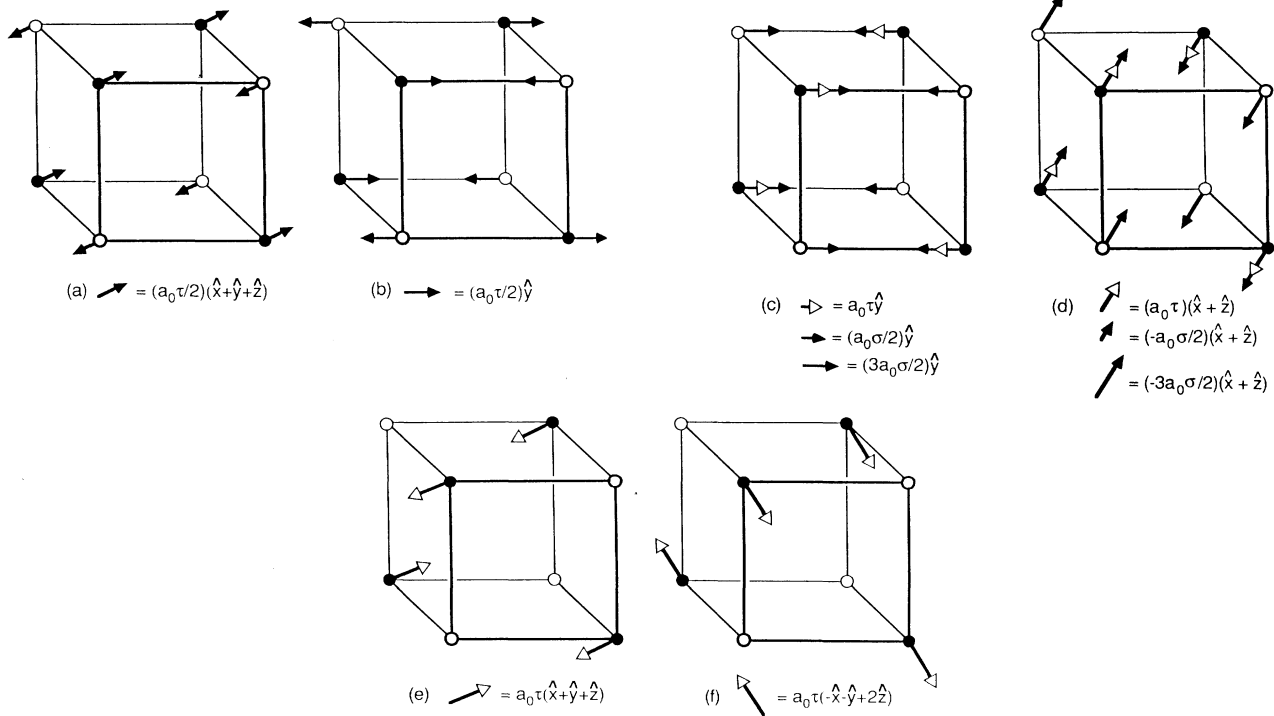


FIG. 4. For each family of zero-strain local-mode configurations, labeled (a)–(f) as in Table I, the type of ionic configurations for which total energies are calculated is shown. These ionic configurations are constructed according to the symmetry of the corresponding local-mode configuration, as described in the text. Open and solid circles here represent Ge and Te ions, respectively. For (a), (b), (e), and (f) a fixed τ corresponds to a single ionic configuration. For (c) and (d), the requirements imposed by symmetry are less stringent and a one-dimensional space of ionic configurations, parametrized by σ , corresponds to fixed τ .

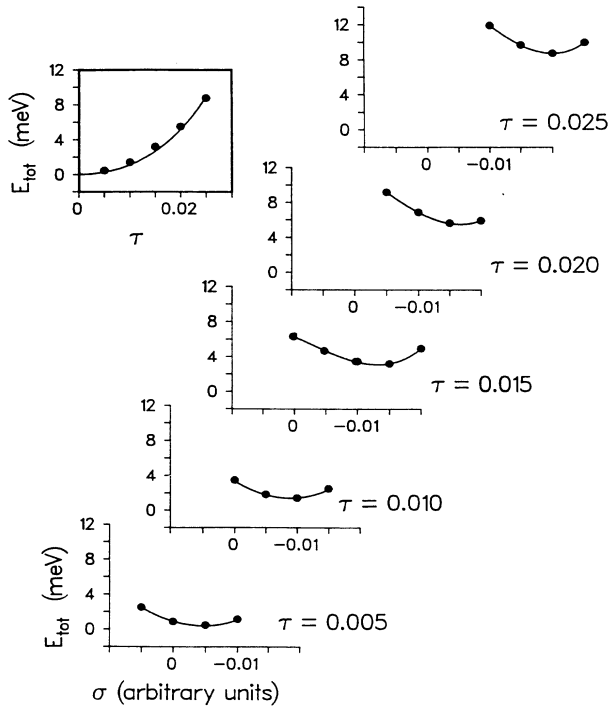


FIG. 5. For each member of a family of local-mode configurations, parametrized by τ , the space of corresponding ionic configurations of same translational and point symmetry, parametrized by σ , is searched for the minimum energy, which is assigned to the local-mode configuration (inset). For the longitudinal tetragonal family shown here, the corresponding space is one dimensional. Energies are given relative to the rocksalt structure minimum in meV per atom.

included through the local density approximation using the Ceperley-Alder-Perdew-Zunger parametrization.²⁷ Eigenfunctions are expanded in a plane-wave basis with energy cutoff $E_1=10.5$ Ry, and Löwdin perturbation theory²⁸ is used to include the effect of plane waves up to $E_2=16.5$ Ry. Brillouin zone averages are performed using Monkhorst-Pack special \mathbf{k} -point sets.²⁹ The specific details of the \mathbf{k} -point sets for each configuration are included in Table I. In previous work⁴ we have seen that this gives extremely good basis-set convergence, and the error is dominated by \mathbf{k} -point sampling. Computations were done on an IBM 370/4381 with 8-byte word length.

Details of the minimization procedure relating local-mode configuration energies in families (c) and (d) to ionic

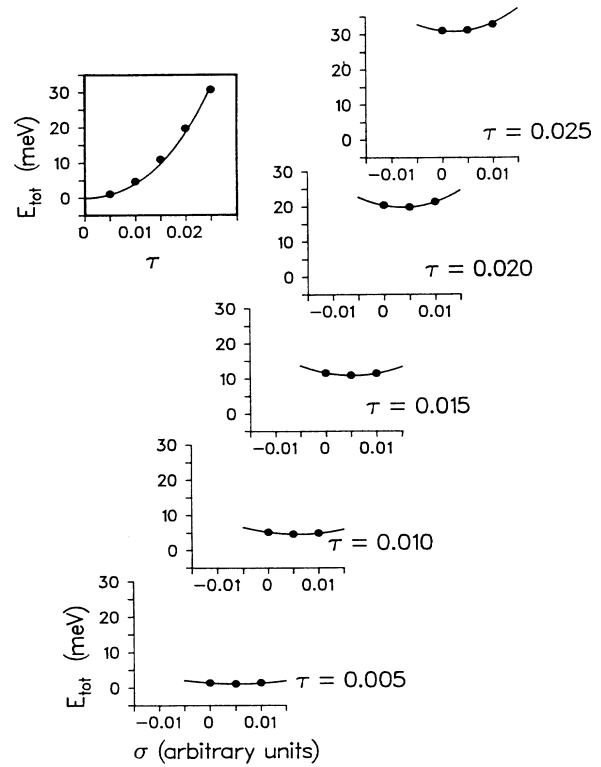


FIG. 6. Same as Fig. 5 for the transverse tetragonal family (d).

configuration energies are shown fully in Figs. 5 and 6. The results for the energies of all the zero-strain local-mode configurations are shown in Fig. 7. Energies of configurations including strain are shown in Fig. 8. We include the results for smaller \mathbf{k} -point sets in Fig. 7 to demonstrate the convergence. With the cutoffs used, energy curvatures are determined to about 10% accuracy.

The model Hamiltonian parameters were obtained through a two-step fitting process. First, the zero-strain coefficients were fit to the zero-strain local-mode configuration energies, measured relative to the energies at $\tau=0$. Then, the strain parameters were fit to the energies of strained configurations, holding the zero-strain coefficients fixed and letting the a_0 in the definition of ξ vary with $\vec{\epsilon}$. The quality of the fit can be seen from the solid lines in Figs. 7 and 8. The resulting parameters are given in Table II.

TABLE II. Model Hamiltonian parameters for GeTe (eV).

	On site	Intersite	Elastic	Coupling
A	59.3	a_1 6.08	C_{11} 29.7	g_0 167
u_0	8.73×10^3	a_2 10.5	C_{12} 0.12	g_1 420
v_0	4.12×10^3	a_3 4.38	C_{44} 5.75	g_2 134
D	7.32×10^5	$b_1 + 2b_2$ 42.0		
E	2.36×10^7			

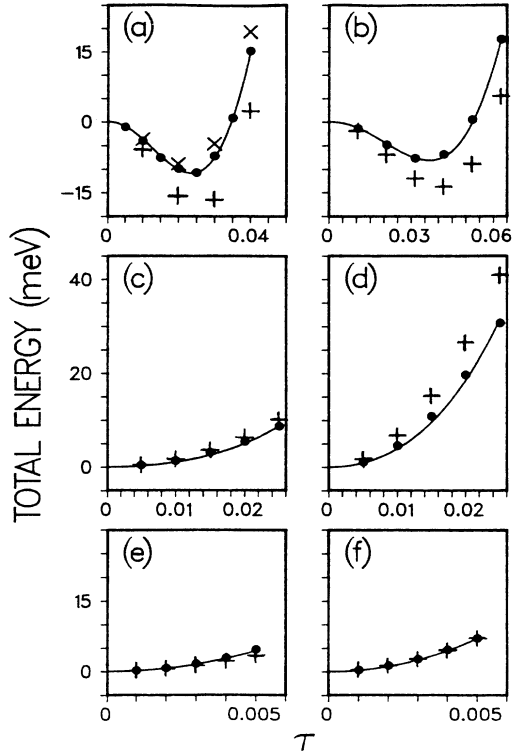


FIG. 7. Calculated local-mode configuration energies, given relative to the rocksalt structure minimum in meV per atom. Solid lines show fit using model Hamiltonian parameters given in Table II. The energies for six families of local-mode configurations with zero strain are shown—longitudinal and transverse: (a),(b), fcc; (c),(d), tetragonal; and (e),(f), rhombohedral. The crosses show the results of calculations with the smaller \mathbf{k} -point sets given in Table I.

IV. STATISTICAL MECHANICS

Given this microscopic Hamiltonian, the transition temperature and critical properties follow from the evaluation of the partition function. A systematic approach begins with a Hubbard-Stratonovich transformation on the parti-

$$\begin{aligned}
 \beta H_{\text{HS}} = \int d^3r \left[r_0(T - T_0) |\phi(\mathbf{r})|^2 + |\nabla\phi(\mathbf{r})|^2 \right] / 2 \\
 + \left[\sum_{\alpha} f(\partial_{\alpha}\phi_{\alpha})^2 - \sum_{\substack{\alpha, \beta \\ \alpha \neq \beta}} h(\partial_{\beta}\phi_{\alpha})(\partial_{\alpha}\phi_{\beta}) \right] / 2 + \bar{u} |\phi(\mathbf{r})|^4 + \bar{v} \sum_{\alpha} \phi_{\alpha}(\mathbf{r})^4 + \mathcal{O}(\phi^6) \\
 + (6\pi^2)^{-1} \left[\bar{Z}_3 \sum_{\alpha} e_{\alpha\alpha}(\mathbf{r}) / 3 + \bar{C}_{11} \sum_{\alpha} e_{\alpha\alpha}^2(\mathbf{r}) / 2 + \bar{C}_{12} \sum_{\substack{\alpha, \beta \\ \alpha \neq \beta}} e_{\alpha\alpha}(\mathbf{r}) e_{\beta\beta}(\mathbf{r}) / 2 \right. \\
 + \bar{C}_{44} \sum_{\substack{\alpha, \beta \\ \alpha \neq \beta}} e_{\alpha\beta}^2(\mathbf{r}) - \bar{g}_0 \sum_{\alpha} e_{\alpha\alpha}(\mathbf{r}) |\phi(\mathbf{r})|^2 / 3 - \bar{g}_1 \sum_{\substack{\alpha, \beta \\ \alpha < \beta}} e_{\alpha\beta}(\mathbf{r}) \phi_{\alpha}(\mathbf{r}) \phi_{\beta}(\mathbf{r}) \\
 \left. - \bar{g}_2 \sum_{\alpha} e_{\alpha\alpha}(\mathbf{r}) [\phi_{\alpha}(\mathbf{r})^2 - |\phi(\mathbf{r})|^2 / 3] \right].
 \end{aligned}$$

In anticipation of the RG analysis below, we have taken the continuum limit, defined the length scale so that the Brillouin zone is approximated by a sphere of radius 1, and normalized the $\phi(\mathbf{r})$ so the $|\nabla\phi(\mathbf{r})|^2$ term has coefficient $\frac{1}{2}$.

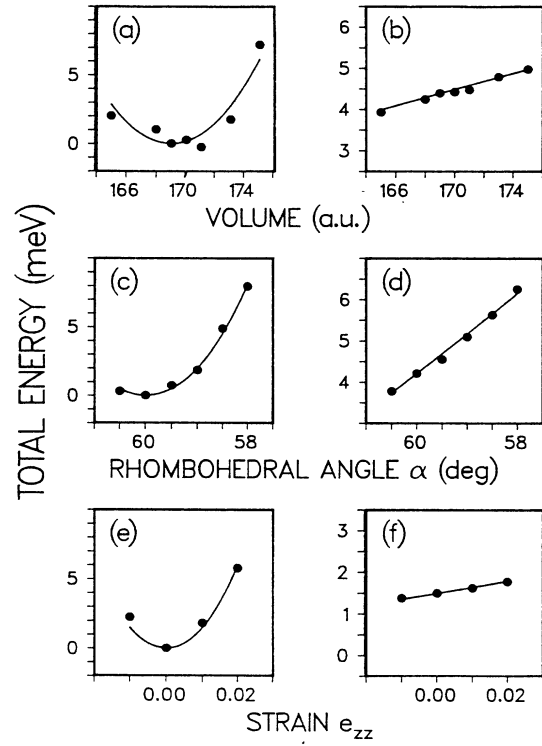


FIG. 8. Same conventions as Fig. 7. On the right, energies of configurations which include strain are shown: (a), (c), and (e) are pure strain distortions, while (b), (d), and (f) show $E(e, \tau=0.01) - E(e, \tau=0.00)$ which determines the order-parameter strain coupling. Note the differences in energy scale among (a), (c), (e); (b), (d), (f), and Fig. 7.

tion function

$$Z = \int [\Pi(d\xi_i)] \mathcal{D}\vec{e}(\mathbf{r}) \exp[-\beta H_{\text{mod}}(\{\xi_i\}, \{\vec{e}(\mathbf{r})\})],$$

to introduce a field ϕ_i which couples linearly to the order parameter. The trace over ξ_i is expanded in ϕ_i and $\vec{e}(\mathbf{r})$ to give a functional of the same form as the original Hamiltonian:

TABLE III. Coefficients in the functional $\beta H_{\text{HS}}(\{\xi_i\}, \{e(\mathbf{r})\})$

On site		Intersite		Elastic		Coupling	
r_0	3.68 (eV)^{-1}	f	0.00	\bar{C}_{11}	1.03×10^3	\bar{g}_0	19.5
$k_B T_0$	669 K	h	0.10	\bar{C}_{12}	3.72	\bar{g}_1	57.5
\bar{u}	0.0175			\bar{C}_{44}	194	\bar{g}_2	17.5
\bar{v}	0.0133			\bar{Z}_3	-5.75		

All the coefficients except r_0 , f , and h , which arise from the quadratic intersite coupling, are now functions of single-site traces (and thus of β):

$$\langle p(\xi) \rangle = \frac{\int d^3 \xi \exp \left[-\beta \left[A |\xi|^2 + u_0 |\xi|^4 + v_0 \sum_{\alpha} \xi_{\alpha}^4 + D |\xi|^6 + E |\xi|^8 \right] \right] p(\xi)}{\int d^3 \xi \exp \left[-\beta \left[A |\xi|^2 + u_0 |\xi|^4 + v_0 \sum_{\alpha} \xi_{\alpha}^4 + D |\xi|^6 + E |\xi|^8 \right] \right]}.$$

Having manipulated the partition function into a standard functional integral form, we now proceed to evaluate it. The use of the stationary phase approximation leads to a mean-field-theory transition temperature

$$T_{c,\text{MF}} = T_0 - 2\bar{g}_0 \bar{Z}_3 / [3r_0(\bar{C}_{11} + 2\bar{C}_{12})].$$

For GeTe, we find $T_0 = 669$ K while the contribution from strain coupling contributes +4 K, giving $T_{c,\text{MF}} = 673$ K.

An estimate of the correction to the mean-field value of T_c and information about the critical behavior can be ob-

tained through the renormalization group in the ϵ expansion. Since the critical temperature dependence is contained in the vanishing of $T - T_{c,\text{MF}}$, all other coefficients in βH_{HS} are evaluated at $T_{c,\text{MF}}$ and their temperature dependence is neglected in the following discussion. The resulting values of the coefficients in βH_{HS} are given in Table III. This type of compressible three-component model with cubic anisotropy has been studied previously.³⁰ For the present discussion we write the functional in the standard Landau-Ginzburg-Wilson form with $n=3$, $d=3$ and cubic symmetry, including the infinite-range intersite quartic couplings generated by integrating out the homogeneous strain. This leads to

$$\begin{aligned} \beta H_{\text{LGW}} = & \int d^3 r \left[r_0 (T - T_{c,\text{MF}}) |\phi(\mathbf{r})|^2 + |\nabla \phi(\mathbf{r})|^2 / 2 + u |\phi(\mathbf{r})|^4 + v \sum_{\alpha} \phi_{\alpha}(\mathbf{r})^4 \right. \\ & \left. + O(\phi^6) + \left[f \sum_{\alpha} (\partial_{\alpha} \phi_{\alpha})^2 - h \sum_{\substack{\alpha, \beta \\ \alpha \neq \beta}} (\partial_{\beta} \phi_{\alpha})(\partial_{\alpha} \phi_{\beta}) \right] / 2 \right] \\ & + \int d^3 r \int d^3 r' \left[w_0 \sum_{\alpha} \phi_{\alpha}(\mathbf{r})^2 \phi_{\alpha}(\mathbf{r}')^2 + w_1 \sum_{\substack{\alpha, \beta \\ \alpha < \beta}} \phi_{\alpha}(\mathbf{r})^2 \phi_{\beta}(\mathbf{r}')^2 + w_2 \sum_{\substack{\alpha, \beta \\ \alpha < \beta}} \phi_{\alpha}(\mathbf{r}) \phi_{\beta}(\mathbf{r}) \phi_{\alpha}(\mathbf{r}') \phi_{\beta}(\mathbf{r}') \right]. \end{aligned}$$

In analyzing this model, we neglect the higher-order anharmonicities and the anisotropic components of the gradient terms since these are marginal or irrelevant fields and will modify the flows significantly only in extreme cases. Thus we consider the differential recursion relations to first order in $\epsilon = 4 - d$ in the six-dimensional parameter space $r = r_0(T - T_{c,\text{MF}})$, u , v , w_0 , w_1 and w_2 :

$$dr/dl = 2r + (8\pi^2)^{-1}(20u + 12v + 4w_0 + 4w_1)/(1+r),$$

$$du/dl = u - (8\pi^2)^{-1}u(44u + 24v)/(1+r)^2,$$

$$dv/dl = v - (8\pi^2)^{-1}v(36u + 48v)/(1+r)^2,$$

$$dw_0/dl = w_0 - (8\pi^2)^{-1}(24w_0u + 8w_1u + 24w_0v + 4w_0^2)/(1+r)^2,$$

$$dw_1/dl = w_1 - (8\pi^2)^{-1}(32w_1u + 8w_0u + 24w_1v + 2w_1^2 + 4w_0w_1)/(1+r)^2,$$

$$dw_2/dl = w_2 - (8\pi^2)^{-1}(8w_2u + 2w_2^2)/(1+r)^2.$$

By iterating the recursion relations numerically, we examine the changes in the flows as the system moves along the line in parameter space according to the physical temperature T , and find a shift in T_c of -16 K, yielding $T_c = 657$ K.

An analogous treatment of the nearest-neighbor Ising model on a face-centered-cubic lattice gives a shift in T_c of -14%, comparable to that of -18% obtained from numerical studies³¹ in $d=3$. The smaller shift in the

present case results from smaller ratios of the fourth-order couplings to r_0 , as determined by the several independent microscopic coupling constants. To lowest order, the strain-related fluctuation contribution to the shift in T_c can be estimated by mapping to an effective cubic-anisotropy model³¹ $\bar{r} = r + (2\pi^2)^{-1}(w_0 + w_1)$, $\bar{u} = u$, $\bar{v} = v$, which shows that at this level, the shift of 0.35 K is independent of w_2 . In fact, in the present case higher-order effects are also important since comparison of the full flows with those in which we set $w_i = 0$ yields a slightly larger contribution of 3 K.

This RG analysis can also be used to understand the observed first-order character of the transition. At the fixed points of the pure cubic-anisotropy model³² ($w_i = 0$), the w_i are relevant. There are new fixed points with $w_i^* > 0$, but these are not accessible to flows starting in the $w_i < 0$ region of parameter space, as in the present case where $w_0 = -2.71 \times 10^{-3}$, $w_1 = -3.83 \times 10^{-4}$, and $w_2 = -3.60 \times 10^{-2}$. The resulting runaway behavior of the strain-generated couplings is associated in principle with the occurrence of a first-order transition. To see that this runaway, particularly in w_2 , provides a plausible mechanism for the observed character of the transition, consider that within mean-field theory, the effect of the strain coupling is to shift the effective values of (u, v) towards the mean-field phase boundary $u_{\text{eff}} + v_{\text{eff}}/3 = 0$, from (0.018, 0.013) to $(-6.1 \times 10^{-4}, 0.028)$. This substantial shift suggests that though the transition within mean-field theory is still second order, the strain effects could be large enough to produce an observable discontinuity within RG, and thus the transition is fluctuation-driven first order.

V. DISCUSSION AND CONCLUDING REMARKS

Here we review the calculation to see where important approximations and calculational inaccuracies enter, and to separate the features which are special to the GeTe transition from more widely applicable aspects.

We started by assuming that the transition could be described by a purely ionic Hamiltonian expanded about the prototype structure. Although models have been proposed in which the near-band-gap electronic states are the direct source of the temperature dependence,^{33,34} it seems unlikely that this effect could be significant compared to the lattice anharmonicity in the case of GeTe. Defining a local-mode variable, we formally obtained a model Hamiltonian that exactly reproduced the thermal behavior of the original. Then we approximated the model by a truncated expansion—local anharmonicity, no intersite interactions beyond second neighbor, lowest-order local-mode-strain coupling—with no temperature dependence in the coefficients. Because the definition of the local-mode variable and truncation of the model Hamiltonian (which is important in determining the quantitative accuracy of the model) depends on the physics of the GeTe transition, the details of this part of the procedure would need to be rethought when applied to other systems. In particular, although the local-mode approximation can be used to obtain model Hamiltonians for both displacive and order-disorder

structural transitions,¹⁸ the large local anharmonicity in the latter case probably implies that nonlocal anharmonic terms must also be included for a good quantitative description. Therefore this approach is generally feasible only for transitions, like that in GeTe, which have displacive character.

In contrast, once we have obtained the numerical form of the model, the statistical mechanical analysis depends mainly on the universality class of the transition. The dropping of terms from H_{LGW} and the validity of techniques such as the ϵ expansion rely less on the physics of GeTe and are more subject to systematic improvement than the approximations in the form of H_{mod} . For example, the fluctuations could be described using the full Green's function instead of its gradient expansion, the analysis could be carried to higher order in ϵ , and the higher-order anharmonicities, anisotropic fluctuations, and the terms generated by the inhomogeneous strains, could be included explicitly in the recursion relation analysis. In fact, to first order in ϵ the sixth-order anharmonicities can be included in the analysis simply by introducing effective values of u and v .³⁵ For the zero-strain coupling case, we find $(u_{\text{eff}}, v_{\text{eff}})$ shifts only slightly, from (0.018, 0.013) to (0.013, 0.011), so that this correction cannot account for the observed first-order behavior.

The most important calculational errors enter via the total-energy calculations. As discussed in Sec. IV, k-point convergence makes the largest contribution to errors at the level of ionic configuration energies, resulting in uncertainty in the quadratic coefficients in H_{mod} of about 10%. Propagation through to T_c shows that the error in T_c is slightly sublinear in the uncertainty in the coefficients. At the level of H_{mod} , we also were unable to separate b_1 and b_2 . Since we expect both of these to be positive, we introduce $\nu \in [0, 1]$ with $b_1 = \nu(b_1 + 2b_2)$, $b_2 = (1 - \nu)(b_1 + 2b_2)/2$. For the RG analysis, we chose $\nu = 0.37$ which is a reasonable value in view of the lack of strong anisotropy of the first-neighbor interactions and has the additional advantage that $f = 0$. If we had included f explicitly in the RG analysis, it would be possible to obtain quantitative bounds on $T_c(\nu)$. However, since $T_{c,\text{MF}}$ depends only on $b_1 + 2b_2$, T_c should be fairly insensitive to ν . With the above considerations, we make an estimate of the error in T_c to obtain a final answer of 657 ± 100 K.

Aside from T_c and the character of the transition, a number of other properties derivable within this framework could be compared with experiment. Experimentally observable quantities related to the strain include dT_c/dP , elastic constants and their discontinuity at the transition, and the discontinuity of the thermal expansion coefficient at the transition. These provide information about the order-parameter strain couplings in the system and could be calculated using our approach, although a more refined treatment of the strain degrees of freedom would be required than that given here.

In summary, we have studied the phase transition of GeTe completely *ab initio*, predicting $T_c = 657 \pm 100$ K. This compares quite favorably with the range of experimental values of 625–700 K. In addition, we find that

the presence of the order-parameter strain coupling moves the system into the fluctuation-driven first-order region of the phase diagram, consistent with experimental indications of a discontinuous transition. This provides an encouraging prospect for future applications of the pseudopotential total-energy method to the calculation of finite-temperature properties of solids.

ACKNOWLEDGMENTS

We acknowledge valuable discussions with A. N. Berker, A. Aharony, M. Kardar, and D. Blankshtein. One of us (K.R.) thanks AT&T Bell Laboratories for support. This work was supported in part by Office of Naval Research Contract No. N00014-86-K-0158.

- ¹J. Ihm, D. H. Lee, J. D. Joannopoulos, and J. J. Xiong, *Phys. Rev. Lett.* **51**, 1872 (1983).
- ²L. L. Boyer and J. R. Hardy, *Phys. Rev. B* **24**, 2577 (1981).
- ³See, for example, references cited in K. M. Rabe and J. D. Joannopoulos, *Phys. Rev. B* **32**, 2302 (1985).
- ⁴K. M. Rabe and J. D. Joannopoulos, *Phys. Rev. B* **32**, 2302 (1985).
- ⁵L. E. Shelimova, N. Kh. Abrikosov, and V. V. Zhdanova, *Russ. J. Inorg. Chem.* **10**, 650 (1965).
- ⁶A. D. Bigava, A. A. Gbedava, E. D. Kunchuliya, S. S. Moiseenko, and R. R. Shvangiradze, *Izv. Akad. Nauk. SSSR, Neorg. Mater.* **12**, 835 (1976) [*Inorg. Mater.* **12**, 708 (1976)].
- ⁷N. Kh. Abrikosov, O. G. Karpinskii, L. E. Shelimova, and M. A. Korzhuev, *Izv. Akad. Nauk. SSSR, Neorg. Mater.* **13**, 2160 (1977) [*Inorg. Mater.* **13**, 1723 (1977)].
- ⁸M. Iizumi, Y. Hamaguchi, K. F. Komatsubara, and Y. Kato, *J. Phys. Soc. Jpn.* **38**, 443 (1975).
- ⁹K. Schubert and H. Fricke, *Z. Naturforsch.* **6a**, 781 (1951); *Struct. Rep.* **15**, 72 (1951); *Z. Metallkd.* **44**, 457 (1953); *Struct. Rep.* **17**, 44 (1953).
- ¹⁰J. N. Bierly, L. Muldawer, and O. Beckman, *Acta. Metall.* **11**, 447 (1963).
- ¹¹T. B. Zhukova and A. I. Zaslavskii, *Kristallografiya* **12**, 37 (1967) [*Sov. Phys.—Crystallogr.* **12**, 28 (1967)].
- ¹²N. Kh. Abrikosov, M. A. Korzhuev, L. A. Petrov, O. A. Teplov, and G. K. Demenskii, *Izv. Akad. Nauk. SSSR, Neorg. Mater.* **19**, 370 (1983) [*Inorg. Mater.* **19**, 334 (1983)].
- ¹³S. I. Novikova, L. E. Shelimova, N. Kh. Abrikosov, V. I. Galyutin, and B. A. Evseev, *Fiz. Tverd. Tela (Leningrad)* **12**, 3623 (1971) [*Sov. Phys.—Solid State* **12**, 2945 (1971)].
- ¹⁴S. I. Novikova, L. E. Shelimova, N. Kh. Abrikosov, and B. A. Evseev, *Fiz. Tverd. Tela (Leningrad)* **13**, 2764 (1972) [*Sov. Phys.—Solid State* **13**, 2310 (1972)].
- ¹⁵S. I. Novikova, L. E. Shelimova, N. Kh. Abrikosov, and O. G. Karpinskii, *Fiz. Tverd. Tela (Leningrad)* **19**, 1171 (1977) [*Sov. Phys.—Solid State* **19**, 683 (1977)].
- ¹⁶S. I. Novikova, L. E. Shelimova, E. S. Avilov, and M. A. Korzhuev, *Fiz. Tverd. Tela (Leningrad)* **17**, 2379 (1975) [*Sov. Phys.—Solid State* **17**, 1570 (1975)].
- ¹⁷N. Kh. Abrikosov, M. A. Korzhuev, and L. E. Shelimova, *Izv. Akad. Nauk. SSSR, Neorg. Mater.* **13**, 1757 (1977) [*Inorg. Mater.* **13**, 1418 (1977)].
- ¹⁸M. E. Lines and A. M. Glass, *Principles and Applications of Ferroelectrics and Related Materials* (Clarendon, Oxford, 1977).
- ¹⁹W. Cochran, *Adv. Phys.* **9**, 387 (1960).
- ²⁰P. W. Anderson, in *Fizika Dielektrikov*, edited by G. Skanavi (Akad. Nauk, Moscow, 1960).
- ²¹M. E. Lines, *Phys. Rev.* **177**, 797 (1969).
- ²²P. B. Littlewood, *J. Phys. C* **13**, 4855 (1980); **13**, 4875 (1980).
- ²³A. Bussmann-Holder, H. Bilz, and P. Vogl, in *Dynamical Properties of IV-VI Compounds*, Vol. 99 of *Springer Tracts in Modern Physics* (Springer, New York, 1983).
- ²⁴M. T. Yin and M. L. Cohen, *Phys. Rev. B* **25**, 7403 (1982).
- ²⁵D. Vanderbilt, Ph.D. thesis, Massachusetts Institute of Technology, 1981.
- ²⁶G. B. Bachelet, D. R. Hamann, and M. Schlüter, *Phys. Rev. B* **26**, 4199 (1982).
- ²⁷D. M. Ceperley, *Phys. Rev. B* **18**, 3126 (1978); D. M. Ceperley and B. J. Alder, *Phys. Rev. Lett.* **45**, 566 (1980); J. Perdew and A. Zunger, *Phys. Rev. B* **23**, 5048 (1981).
- ²⁸P. O. Löwdin, *J. Chem. Phys.* **19**, 1396 (1951).
- ²⁹H. J. Monkhorst and J. D. Pack, *Phys. Rev. B* **13**, 5188 (1976).
- ³⁰T. Natterman, *J. Phys. A* **10**, 1757 (1977); K. K. Murata, *Phys. Rev. B* **15**, 4328 (1977); G. Bender, *Z. Phys. B* **23**, 285 (1976).
- ³¹C. Domb and A. R. Miedema, in *Progress in Low Temperature Physics IV*, edited by C. J. Gorter (North-Holland, Amsterdam, 1964).
- ³²A. Aharony, *Phys. Rev. B* **8**, 4270 (1973); in *Phase Transitions and Critical Phenomena*, edited by C. Domb and M. S. Green (Academic, New York, 1976), Vol. 6, p. 357.
- ³³M. A. Korzhuev, L. I. Petrova, G. K. Demenskii, and O. A. Teplov, *Fiz. Tverd. Tela (Leningrad)* **23**, 3387 (1981) [*Sov. Phys.—Solid State* **23**, 1966 (1981)], and references therein.
- ³⁴V. A. Volkov and Yu. V. Kopaev, *Zh. Eksp. Teor. Fiz.* **64**, 2184 (1973) [*Sov. Phys.—JETP* **37**, 1103 (1981)].
- ³⁵D. Blankshtein and A. Aharony, *Phys. Rev. B* **28**, 386 (1983).